International Journal of Pharmaceutics 545 (2018) 93–100

Contents lists available at ScienceDirect

International Journal of Pharmaceutics

journal homepage: www.elsevier.com/locate/ijpharm

An EPR spin probe study of the interactions between PC liposomes and stratum corneum membranes

Sebastião Antonio Mendanha[a], Jorge Luiz Veira dos Anjos[b], Lorena Maione-Silva[c], Halanna Cristina B. Silva[c], Eliana Martins Lima[c], Antonio Alonso[a,*]

[a] Physics Institute, Federal University of Goiás, GO, Brazil
[b] Physics Department, Federal University of Goiás, Catalão, GO, Brazil
[c] Laboratory of Pharmaceutical Nanotechnology and Drug Delivery Systems, Federal University of Goiás, Goiânia, GO, Brazil

ARTICLE INFO

Keywords:
Flexible liposomes
Spin labels
EPR
Transepidermal drug delivery

ABSTRACT

The electron paramagnetic resonance (EPR) spin labeling methodology was used to analyze the interactions of phosphatidylcholine (PC) liposomal formulations that are commonly used as transepidermal drug delivery systems with stratum corneum (SC) membranes. The lipid dynamics of five liposome formulations were evaluated to study the influences of sorbitan monooleate (Span80), cholesterol, and cholesterol with the charged lipids 2-dioleoyl-3-trimethylammonium-propane (DOTAP) and 1,2-distearoyl-*sn*-glycero-3-phospho-(1′-*rac*-glycerol) (DSPG) on the molecular dynamics of PC vesicles. The EPR spectra of 5-doxyl-stearic acid (5-DSA) showed that the addition of Span80 to the liposomes increased the lipid fluidity, whereas cholesterol had the opposite effect, and the combination of charged lipids and cholesterol did not additionally influence the lipid bilayer dynamics. Fatty acid spin-labeled SC membranes were treated with the liposome formulations, leading to migration of the spin label to the molecular environment of the formulation and the presence of two spectral components representing distinct mobility states. In terms of molecular dynamics, these environments correspond to the lipid domains of the untreated SC and the liposome, indicating a poor interaction between the liposome and SC membranes. However, the contact was sufficient to allow a pronounced exchange of the spin-labeled fatty acid. Our data suggest that flexible liposomes may access the inner intercellular membranes of the SC and facilitate mutual lipid exchange without losing their relative liposomal integrity.

1. Introduction

Many skin drug delivery systems have been used to explore different routes to release drugs in a controlled and directed manner (Pilcer and Amighi, 2010; Sahoo et al., 2013; Malik et al., 2007). In particular, the transepidermal route has become popular since the skin, in addition to presenting a large application surface, has a low drug metabolism (Prausnitz et al., 2004; Prausnitz and Langer, 2008). However, to use the transepidermal route efficiently, the skin barrier function must be altered (in a controlled and reversible manner). This barrier function is conferred by the outermost skin layer, termed the stratum corneum (SC).

Various alternatives have been used to circumvent the SC barrier function. The so-called second-generation transdermal delivery systems use chemical enhancers, noncavitational ultrasounds, and/or iontophoresis to control delivery rates and provide extra functionality to the first-generation systems, which were mainly used to deliver small lipophilic low-dose drugs (Prausnitz and Langer, 2008). Specifically, chemical permeation enhancers have the principal characteristic ability to alter the fluidity of SC lipid bilayers, thus promoting increased drug penetration of the skin (Karande et al., 2005). For example, Narishetty and Panchagnula demonstrated that the use of enhancers, such as oxygen-containing monoterpenes cineole, menthol, a-terpineol, menthone, pulegone, and carvone, increased the *ex vivo* permeation of zidovudine (AZT) through rat skin at concentrations large enough for the drug to reach the bloodstream at therapeutic concentrations (Narishetty and Panchagnula, 2004).

A more complex approach for the use of permeation enhancers is the use of specialized liposomes. The main advantage of this strategy is that liposomes may act as a reservoir for a drug within the skin and, depending on their composition, may also increase the diffusivity of the drug in the skin, cause SC lipid fluidization, increase drug thermodynamic activity or affect the drug partition coefficient, thus increasing drug release into the upper layers of the skin (Sharma et al. 2014).

* Corresponding author.
E-mail address: alonso@ufg.br (A. Alonso).

https://doi.org/10.1016/j.ijpharm.2018.04.057
Received 16 November 2017; Received in revised form 23 April 2018; Accepted 25 April 2018
Available online 26 April 2018
0378-5173/

Among the liposomal formulations used for transepidermal permeation of drugs, so-called flexible liposomes have been highlighted, and several applications of these liposomes have been reported (Duangjit et al., 2014; Benson, 2017; Touitou et al., 2000, Cevc, 2004). This class of liposome has high fluidity and flexibility of its bilayer, and several authors claim that the flexibility of this specialized liposome allows it to reach the lower layers of the skin while essentially intact, thus increasing transepidermal drug penetration (Cevc, 1996; Cevc et al., 1998; Cevc and Vierl, 2010). On the other hand, other authors assert that the constituents of flexible liposomes may act as permeation enhancers, thereby enabling increased drug permeation (Elsayed et al., 2007; Sharma et al. 2014 and references therein). A consensus regarding the actual mechanism of flexible liposome permeation has not been reached in the literature (El Maghraby et al., 2006; El Maghraby et al., 2008).

The electron paramagnetic resonance (EPR) spectroscopy associated with the spin label technique has been used to evaluate the effects of permeation enhancers in the SC. For instance, our group used lipid, proteic and amphiphilic spin labels to quantify the effects of enhancers, such as monoterpenes (Camargos et al., 2010; Anjos et al., 2007; dos Anjos and Alonso, 2008; Camargos et al., 2014; Mendanha et al., 2013, 2017; Moreira et al., 2014), oleic acid (de Queirós et al., 2005), and ethanol (dos Anjos et al., 2007) on the lipid lamellae and SC proteins. SC lipid membranes are very rigid, whereas the lipid bilayer of flexible liposomes containing phosphatidylcholine (PC) and surfactant is very fluid. In this work, we examined whether the mix of flexible liposome components with the lipids of SC membranes to increase their fluidity or if they remain intact in separate structures with mobility states distinct from those of the SC membranes. Thus, we used spin-label EPR spectroscopy combined with spectral simulations to assess the interactions of flexible liposomes and other soybean PCs with SC intercellular membranes. Our results supported the second hypothesis, i.e., the EPR spectra indicated the presence of two lipid environments with different molecular dynamics even though the contact was sufficient to promote spin label transfers between the two types of membrane.

2. Materials and methods

2.1. Chemicals

Soybean PC was purchased from Lipoid (Ludwigshafen, Germany) and 1,2-dioleoyl-3-trimethylammonium-propane (DOTAP) and 1,2-distearoyl-*sn*-glycero-3-phospho-(1′-*rac*-glycerol) (DSPG) were purchased from Avanti Polar Lipids Inc. (Alabaster, USA). The spin label 5-doxyl-stearic acid (5-DSA), sorbitan monooleate (Span80), cholesterol (chol) and sucrose were purchased from Sigma-Aldrich (St. Louis, USA). The other reagents were purchased from Sigma-Aldrich or Merck SA (Rio de Janeiro, Brazil) at the highest available purities.

2.2. Preparation and spin labeling of freeze-dried PC liposomes

The liposomal formulations used in this work were as follows: pure PC, PC:chol at a (4:1) molar ratio, PC:chol:DOTAP (4:1:0.5), PC:chol:DSPG (4:1:0.5) and PC:Span80 (4:1.7). Each formulation was prepared by dissolving PC and other constituents (DSPG, DOTAP, cholesterol and Span80) in chloroform to prepare a film of lipids on the bottom of a glass tube. The organic solvent was evaporated by a stream of gaseous nitrogen, and the films were kept in a vacuum for 12 h. Subsequently, the film containing Span80 was hydrated with a 5.25% ethanolic solution to form multilamellar liposomal suspensions. The other PC films were hydrated with sodium succinate buffer (0.1 M pH 3.0). Sucrose (used as a cryoprotectant) was added to the hydration solution for all formulations at the ratio 1:2.5 (PC:sucrose).

Unilamellar liposomes were obtained after rigorous extrusion using polycarbonate filters with 0.2-μm diameter pores. Subsequently, each sample was frozen at approximately – 20 °C for 24 h and freeze-dried for 24 h (MicroModulyo, Thermo Scientific, USA). The PC:Span80 sample was resuspended in the same 5.25% ethanolic solution, and the other samples were resuspended in succinate buffer. These procedures generated PC liposomes with a diameter of 97.13 ± 0.09 nm, PdI of 0.09 ± 0.01, and elasticity of 4.17 ± 0.14 $mg{\cdot}s^{-1}{\cdot}cm^{-2}$; PC:Span80 liposomes with a diameter of 90.41 ± 3.46 nm, PdI of 0.10 ± 0.01, and elasticity of 23.88 ± 4.16 $mg{\cdot}s^{-1}{\cdot}cm^{-2}$; PC:chol liposomes with a diameter of 170.40 ± 3.58 nm, PdI of 0.13 ± 0.01, and zeta potential of + 4.77 ± 0.15 mV; PC:chol:DOTAP liposomes with a diameter of 190.10 ± 3.55 nm, PdI of 0.18 ± 0.03, and zeta potential of + 50.17 ± 0.59 mV; and PC:chol:DSPG liposomes with a diameter of 173.60 ± 3.11 nm, PdI of 0.10 ± 0.04, and zeta potential of -44.41 ± 4.16 mV. Next, 1 μL of the 5-DSA spin label (previously dissolved in ethanol at 5 μg/mL) was added to each resuspended formulation to obtain spin-labeled liposomes. Finally, 50 μL of the labeled sample was transferred into capillary tubes with an internal diameter of 1 mm, which were flame-sealed for EPR spectroscopy.

2.3. Preparation, spin labeling and treatment of SC membranes

The SC membranes used in this study were obtained from Wistar rats that were less than 24 h old and were prepared according to a protocol that was approved by the Ethics Committee for the use of animals in research at the Universidade Federal de Goiás (protocol number: 022/16) and described by Alonso et al. (de Queirós et al., 2005; Alonso et al., 2003). Neonatal rat and human SC lipid compositions are similar, and an important advantage of using newborn rat skin is that pilosebaceous lipids cannot contaminate the newborn rat epidermis since developing hair structures do not penetrate the SC until the second postnatal day (Elias et al., 1979). In addition, we have been able to prepare rat SC membranes with higher qualities than human membranes; newborn SC membranes are more homogenous and free of contamination from epidermal lipids such as triglycerides, resulting in better-quality EPR spectra and providing more accurate and reproducible results.

To perform the EPR experiments in which the SC must be spin-labeled, the intact SC samples (~2 mg) were first incubated for 30 min at room temperature in an acetate-buffered saline solution (10 mM acetate and 150 mM NaCl, pH 5.1). Then, the hydrated SC membranes were repeatedly rubbed in glass plates containing an aliquot (2 μL) of the 5-DSA probe (dissolved in ethanol at 5 mg/mL). Subsequently, the SC membranes were incubated for 1 h at room temperature in 50 μL of the desired liposomal dispersions. Then, excess liposomal formulations were removed, and the SC membranes were transferred into glass capillary tubes, which were then flame-sealed. Inside the capillary tube, the treated SC was moderately compacted, minimizing the amount of free liposomes incorporated in the EPR samples. All data are presented as the means ± S.D. from at least three independent experiments.

2.4. EPR spectroscopy and spectral simulation

EPR measurements were performed using a Bruker EMX Plus spectrometer (Rheinstetten, Germany) operating in the X-band (approximately 9.4 GHz) with a 4119-HS resonant cavity and the following instrumental parameters: microwave power, 2 mW; modulation frequency, 100 kHz; amplitude of modulation, 1 G; magnetic field scan, 100 G; scan time, 168 s, and detection time constant, 41 ms. All measurements were performed at 25 °C. The best-fit EPR spectra were obtained using the nonlinear least-squares (NLLS) software developed by Freed JH and co-workers (Budil et al., 1996). As in other studies (Mendanha and Alonso, 2015; Alonso et al., 2012), the motion parameter τ_c, i.e., the rotational correlation time, was obtained via the following equation (Berliner, 1976):

$$\tau_c = \frac{1}{6Rbar}, \quad (1)$$

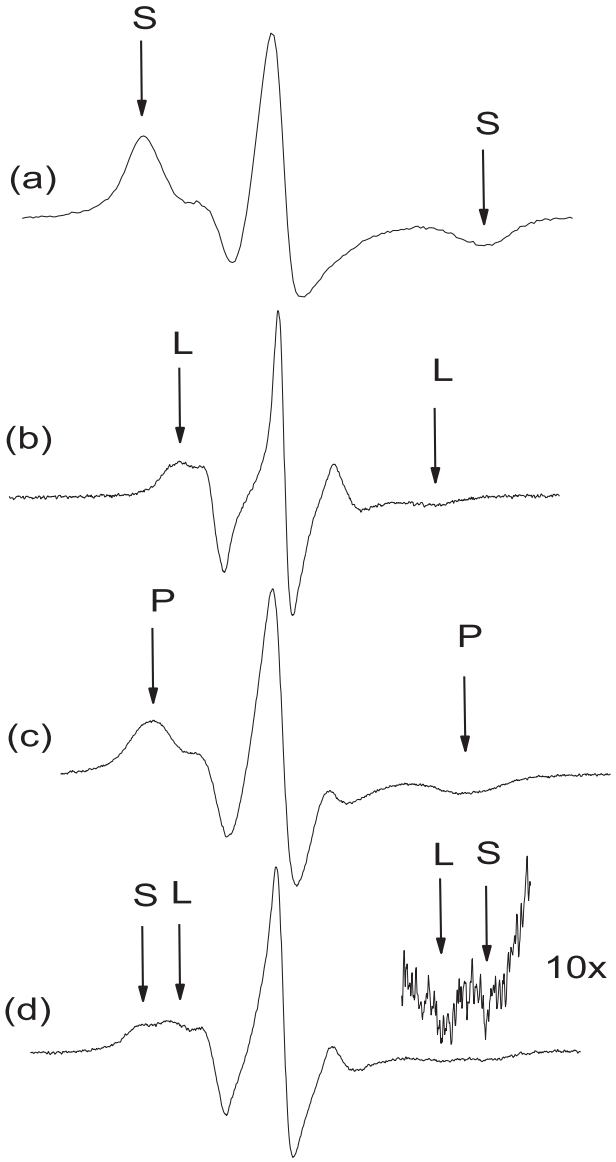

Fig. 1. EPR spectra of the spin label 5-DSA incorporated into intact SC membranes (a) and PC + Span80 liposomes (b). Spectra (c) and (d) are from spin-labeled SC membranes treated with unlabeled Span80 (c) or flexible liposomes (d). Arrows indicate the magnetic field positions where the resonance lines of the components S, P and L are clearly resolved. The intensities of all spectra, represented on the y-axis, are normalized (maximum value equal to 1 in a.u.).

where the rate of rotational Brownian diffusion, R_{bar}, was given as an output from the NLLS program after the best-fit process. In this study, the best-fit spectra were calculated using models containing one or two spectral components. To simulate the spectra of the intact SC membranes, we used the following input parameters for the magnetic tensors g and A: $g_{xx} = 2.0088$, $g_{yy} = 2.0058$, $g_{zz} = 2.0028$, $A_{xx} = 6.6$, $A_{yy} = 6.5$ and $A_{zz} = 33.0$. Conversely, the input parameters used to determine the best-fit of the liposomal formulations were $g_{xx} = 2.0080$, $g_{yy} = 2.0060$, $g_{zz} = 2.0022$, $A_{xx} = 6.6$, $A_{yy} = 6.5$ and $A_{zz} = 29.0$.

3. Results

3.1. EPR analysis of SC-flexible liposome interactions

Fig. 1 shows the EPR spectra of the spin label 5-DSA incorporated into intercellular membranes of intact SCs (a) and the Span80-liposomal formulation (b). To obtain spectra (c) and (d), the SC membranes were spin labeled with 5-DSA and were subsequently treated for 1 h with Span80 (c) or the Span80-liposomal formulation (d). Notably, spectrum 1d clearly comprises two distinct mobility components that could be roughly described as a combination of the 1a and 1b spectra. Thus, the application of Span80 liposomes to the SC membranes caused the liposome formulation to remain relatively stable, indicating that the interaction of the formulation with the SC membranes was small. However, the interaction was sufficient for the spin label to migrate from the SC lipids to the formulation. In contrast, when SC membranes were treated with Span80, only one spectral component was clearly resolved (spectrum 1c), indicating that Span80 was mixed with SC lipids, which increased their mobility. Thus, to evaluate the interactions between the Span80-liposomal formulation and the SC membranes, we performed spectral simulations using models of one or two spectral components to determine the spin label distribution between the two systems (SC lipid matrix and liposome formulation) to assess lipid dynamic changes in each of these two systems.

The spectral simulations using the NLLS software allowed us to fit the experimental spectra using one or two spectral components, with each component representing a spin label population with a characteristic line shape, rotational motion and magnetic parameters. Thus, we used the one-component model to fit the spectra of the intact SC membranes and flexible liposomes, as shown in Fig. 2a and b, respectively. Moreover, the two-component model was applied to fit the spectra of the SC membranes treated with the flexible-liposomal formulation (Fig. 2c). Hereafter, the term spectral component S (CS) will be used to represent the fraction of the spin labels that are structured in an environment similar to that of the intercellular membranes of the intact SC membranes. Thus, to simulate CS in the composed spectrum, we used the parameters obtained for the best-fit spectrum of the intact SC membranes as input parameters, including the rotational correlation time, τ_c, and the eigenvalues of the magnetic tensors g and A for intact SC membranes, as described in the previous section. Similarly, the spectral component L (CL) was denoted by the fraction of spin labels located in an environment similar to those of the liposome bilayers, and the input parameters used to simulate this component in the composed spectrum were those obtained from the best-fit spectrum for the liposome formulation (τ_c and the eigenvalues of the magnetic tensors g and A for the liposomal formulations). The motion parameter τ_c and the fractions of the spin labels in each component (N_S and N_L) were obtained from the two-component spectral simulations as output data. The best-fit parameters are those that lead to the best convergence between the experimental and theoretical spectra, and the quality of convergence was monitored by the correlation coefficient provided by the fitting program (Budil et al., 1996).

Fig. 3 shows five different combinations of CS and CL and their respective best-fit line shape outputs, along with the relative CS probe population (N_S) and the motion parameter of the spin label 5-DSA structured in the SC intercellular membranes treated with the PC-Span80-liposomal formulation. The best-fit spectrum from Fig. 3a was obtained using the one-component model, and only the CS or CL parameters were employed as the inputs for the spectral simulation. The simulation parameters were set as free to vary during the best-fit process. thus, a completely different line shape profile was obtained with an associated motion parameter τ_c representing neither the CS nor the CL component. This result suggests that the best-fit of the SC + flexible-liposomal formulation experimental spectrum will be obtained from a combination of CS and CL or from a mixture of two other different components. The best-fit spectrum shown in Fig. 3b was obtained with the CS and CL component parameters as inputs, but these parameters were set to remain fixed during the spectral simulation. This type of simulation allows variations of only the relative spin probe populations of the two components. This process resulted in an unsatisfactory best-fit spectrum with a high contribution of the CS relative spin label population (N_S), reaching ~75%. The best-fit spectrum of Fig. 3c was obtained using the CS and CL input parameters, but the

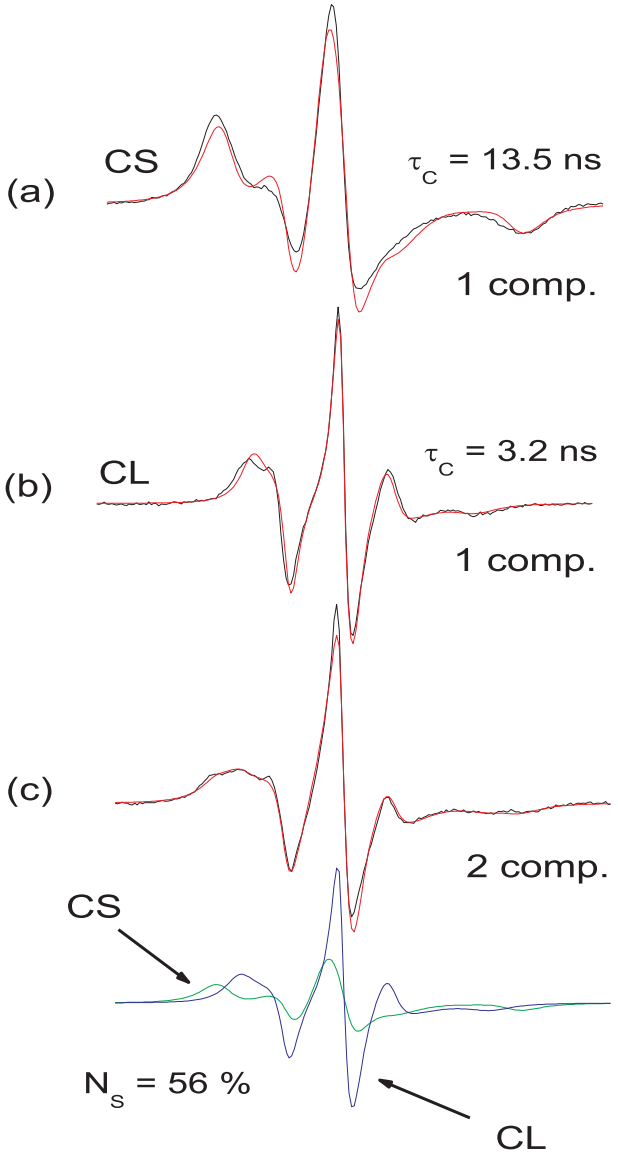

Fig. 2. Illustration of how the components CS and CL were obtained. The black lines represent the experimental EPR spectra of the 5-DSA spin label structured into the SC membranes (a), flexible liposomes (b) and SC + flexible liposomes (c). The red lines represent each best-fit spectrum obtained with the NLLS software. Spectra 2a and 2b were fitted using the one-component model, and the best fits were denoted by CS and CL, respectively. Spectrum 2c was fitted using the two-component model, and the red line is a combination of the CS (green) and CL (blue) lines. The EPR parameter τ_c is the rotational correlation time, which is indicated for each component and is used here as a measure of the microenvironment molecular dynamics. N_S represents the fraction of spin probes that are structured into the SC intercellular membranes. The intensities of the experimental spectra a, b and c, represented on the y-axis, are normalized. (For interpretation of the references to colour in this figure legend, the reader is referred to the web version of this article.)

parameters were free to vary during the fitting process. For this combination, an acceptable best-fit spectrum was found, but the parameter τ_c of the less mobile component (CS-like) was approximately 12 ns greater than the initial value of this component. However, the τ_c parameter associated with CL was found to be the same as that of the isolated liposomes. In the CS/CL combination used to obtain the best-fit spectrum of Fig. 3d, CS remained fixed and CL was set as free to vary. This combination resulted in the best convergence of the experimental and theoretical spectra. The N_S population was found to be approximately 60%, and the τ_c of CL varied by 0.5 ns from that found for the isolated liposomes. Finally, for the best-fit spectrum of Fig. 3e, a CS/CL combination was used with CS set as free to vary and CL set as fixed. The convergence between the theoretical and experimental spectra was not good in the region with a low magnetic field, and the τ_c value was also greater than that obtained for the SC membranes (13.5 ns, Fig. 2).

The above analysis using five simulation approaches clearly showed that the SC + Span80 liposome spectrum should be fit by a combination of fixed CS and free CL spectral components. In our analysis, we considered not only the general convergence between the theoretical and experimental spectra but also the details of the line profile in the region with a high magnetic field, wherein the resonance lines from the SC membranes and flexible liposomes have better resolutions, as shown in Fig. 1. Moreover, the line profile in the high magnetic field region is strongly associated with the value of the motion parameter τ_c (Berliner, 1976).

3.2. Molecular dynamics of liposomal formulations

To further examine the detailed interactions of the flexible liposomes with SC membranes, we also analyzed the effects of variations on the formulation compositions. In addition to the Span80-PC formulation, we also studied pure PC, chol-PC, chol-DOTAP-PC, and chol-DSPG-PC liposomes. Fig. 4 shows the most representative experimental spectra and the respective best-fit theoretical lines of the spin label 5-DSA incorporated into the five liposomal formulations. For each experimental spectrum, the outer hyperfine splitting parameter $2A_{||}$, that is, the separation in magnetic field units between the outer hyperfine resonance lines from the spectrum, could be defined (Fig. 4a). As in previous studies (de Queirós et al., 2005; Alonso et al., 2012), the $2A_{||}$ parameter was used to assess the molecular dynamics of the 5-DSA spin labels. Similar to the rotational correlation time τ_c, large $2A_{||}$ values indicate a less restricted molecular motion of the spin probe. Although the measured $2A_{||}$ and τ_c values of the 5-DSA probe structured in the rigid and ordered SC intercellular membranes were of 62.1 G and 13.5 ns (the spectrum from Fig. 2a), respectively, the values of 44.6 G for $2A_{||}$ and 3.2 ns for τ_c were found for the liposome formulation (PC + Span80) (Fig. 4b). The values of the rotational correlation time τ_c (Fig. 4) indicated that the degree of molecular dynamics of the 5-DSA spin probe incorporated into the studied liposome formulations follows the relationship (PC + Span80) > (pure PC) > (PC + chol) = (PC + chol + DOTAP) = (PC + chol + DSPG). This relationship suggests that the addition of Span80 (spectrum 4b) to the PC bilayers increased the lipid fluidity, while the addition of cholesterol (spectrum 4c) reduced the lipid fluidity (increase of 1.5 G in $2A_{||}$ and ~0.5 ns in τ_c) when compared with that of the pure PC liposomes (spectrum 4a). Moreover, the addition of charged lipids (positive for DOTAP and negative for DSPG) and cholesterol did not cause significant changes in the values of $2A_{||}$ and τ_c.

3.3. Liposome-SC membrane interactions

Based on the results described above and the analysis of the magnetic and motion parameters for SC membranes and liposome bilayers, the best combinations of the CS and CL components for fitting the spectra of the 5-DSA spin probe incorporated into the SC lipids treated with the five liposomal formulations used in this study are shown in Fig. 5. Surprisingly, in all cases, the simulation strategy of keeping CS fixed and CL free generated the best-fit spectra. Specifically, discrete variations were observed in both the CS and CL motion parameter values, indicating that during treatment, some lipid exchange occurred between the SC membranes and liposomes, but the exchange was not sufficient for a significant change in the environment of the spin label. In fact, the spin labels that were previously structured into the intercellular SC membranes were transferred to the lipid bilayers of each liposomal formulation. The overview of Fig. 5 indicates that the partition of CS and CL was slightly imbalanced in favor of the CS component for PC-Span80 liposomes.

To further examine the lipid exchange between the SC membranes

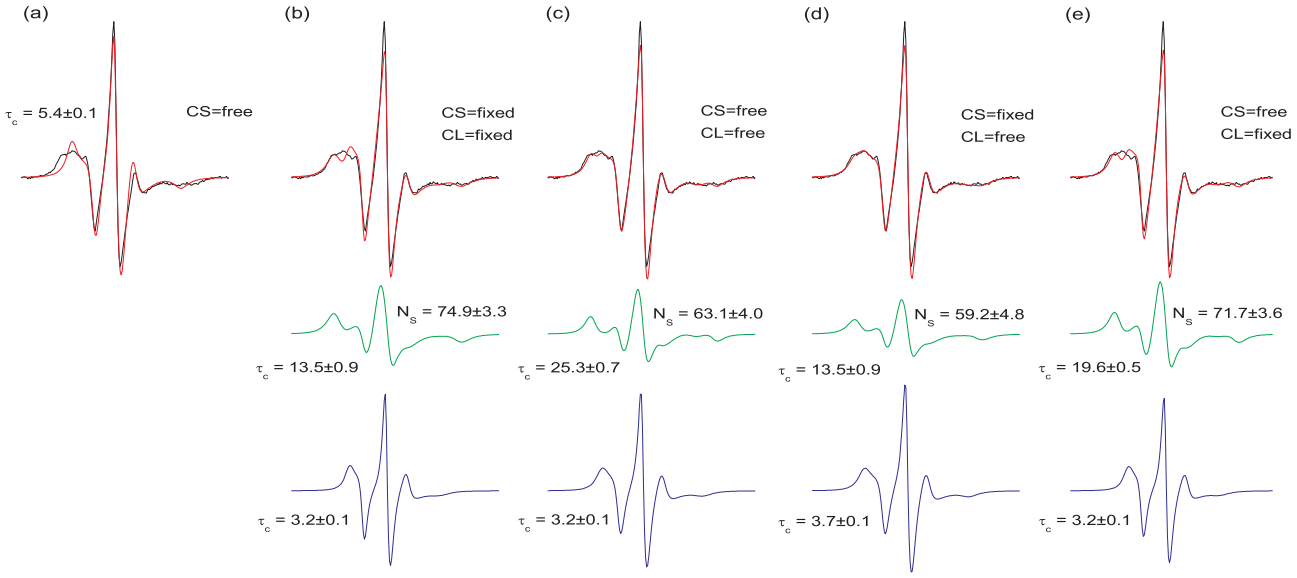

Fig. 3. EPR experimental spectrum (black lines) of the 5-DSA spin label previously structured into SC intercellular membranes treated with unlabeled flexible liposomes. The experimental 5-DSA spectrum was fitted using the same inputs (red lines). Spectrum 3a was fitted using the one-component model, and spectra 3b to 3f were fitted using the two-component model with different combinations of CS and CL. The input parameters were kept fixed or left free to vary in the spectral simulation depending on the CS/CL combination. The green and blue lines represent the spectral components S (spin labels that are structured into the SC membranes) and L (spin labels that are structured into the liposomal formulations bilayers), respectively. N_S indicates the fraction of the spin labels incorporated into the SC, and τ_c is the rotational correlation time of each component. The total magnetic field range used for all spectra was 100 G. The intensities of the experimental spectra a–e, represented on the y-axis, are normalized. (For interpretation of the references to colour in this figure legend, the reader is referred to the web version of this article.)

and the formulations, we performed experiments with an inverse labeling process. Fig. 6 shows the experimental spectra and their respective best-fit curves for the 5-DSA spin probe incorporated into the liposomal formulations, which were subsequently applied to the unlabeled SC membranes. After 1 h of incubation, excess formulations were removed, and the SC-formulation samples were transferred into

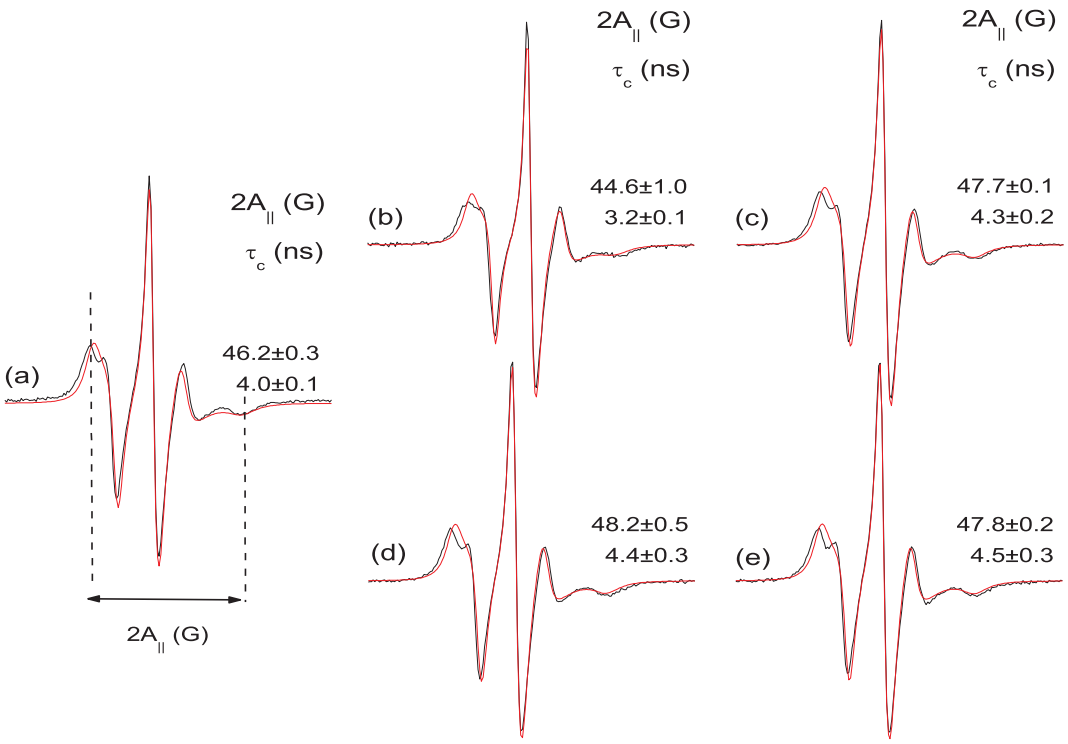

Fig. 4. Experimental (black line) and best-fit (red line) EPR spectra of the 5-DSA spin label structured into pure PC (a), PC + Span80 (b), PC + chol (c), PC + chol + DOTAP (d) and PC + chol + DSPG liposomes (e). All spectra were fitted using the one-component model. The values of the rotational correlation time (τ_c) and the maximum hyperfine splitting parameter ($2A_{||}$) are indicated for each spectrum. Spectrum 4e illustrates how the $2A_{||}$ parameter is calculated from the experimental line. The intensities of all spectra, represented on the y-axis, are normalized. (For interpretation of the references to colour in this figure legend, the reader is referred to the web version of this article.)

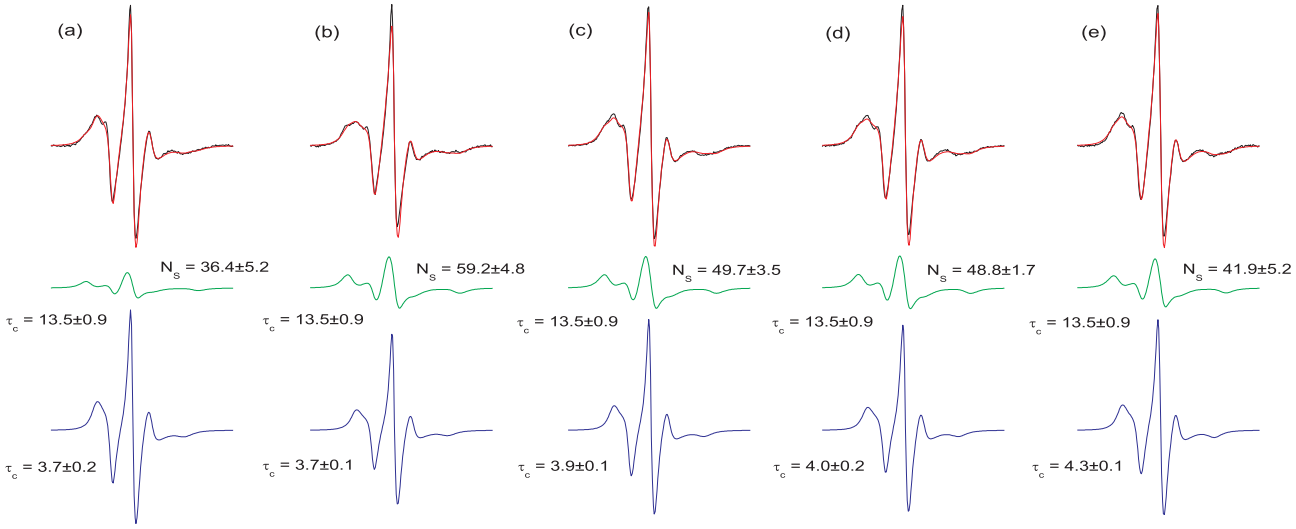

Fig. 5. Experimental (black line) and best-fit (red line) EPR spectra of the 5-DSA spin label previously structured into SC intercellular membranes treated with several unlabeled liposomal formulations: pure PC (a), PC + Span80 (b), PC + chol (c), PC + chol + DOTAP (d), and PC + chol + DSPG (e). All experimental spectra were fitted using the two-component model with the CS input parameters fixed and the CL parameters free to vary during the spectral simulations. The green lines represent the spectral component S, and the blue lines represent the spectral component L. N_S indicates the fraction of the spin labels incorporated into SC membranes, and τ_c represents the rotational correlation time of each component. The total magnetic field range used for all spectra was 100 G, and the intensities of the experimental spectra a–e (on the y-axis) are normalized. (For interpretation of the references to colour in this figure legend, the reader is referred to the web version of this article.)

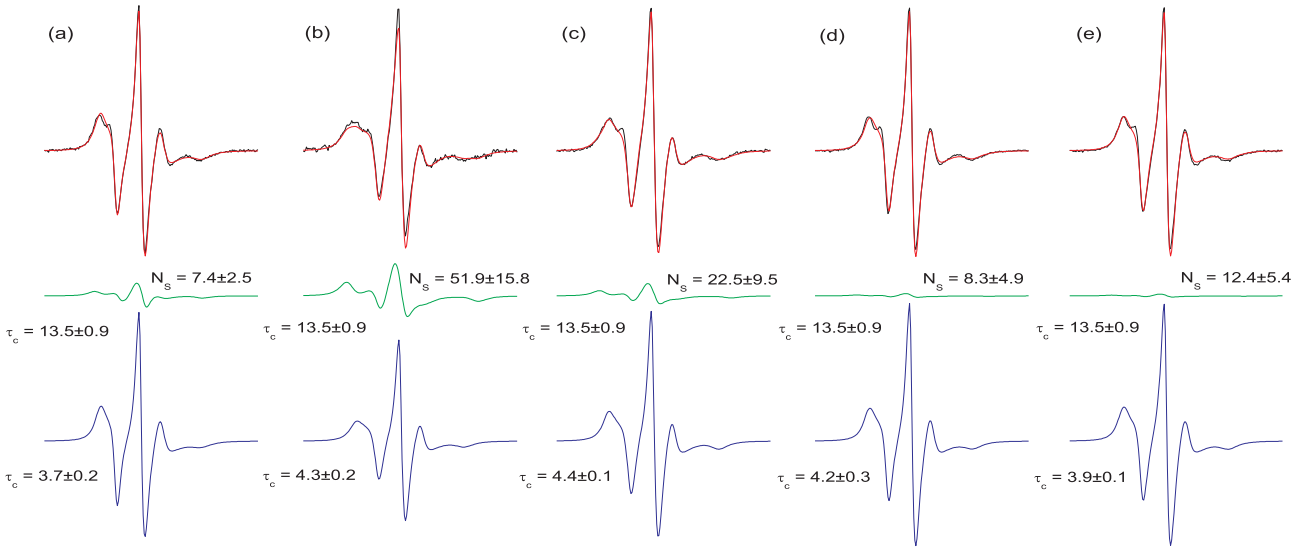

Fig. 6. Experimental (black line) and best-fit (red line) EPR spectra of unlabeled SC membranes treated with the following 5-DSA-labeled liposomes: pure PC (a), PC + Span80 (b), PC + chol (c), PC + chol + DOTAP (d) and PC + chol + DSPG (e). All experimental spectra were fitted using the two-component model with the CS input parameters fixed and the CL parameters free to vary during the spectral simulations. The green lines represent the spectral component S, and the blue lines represent the spectral component L. N_S indicates the fraction of the spin labels incorporated into the SC membranes, and τ_c represents the rotational correlation time of each component. The magnetic field range used in each EPR spectrum was 100 G, and the intensities of the experimental spectra a–e (on the y-axis) are normalized. (For interpretation of the references to colour in this figure legend, the reader is referred to the web version of this article.)

capillary tubes for EPR measurements. To simulate the EPR spectra for these samples, the CS and CL combinations were applied as previously described, and the most acceptable output theoretical spectra are shown (Fig. 6) with their respective motion parameters. Again, the simulation strategy of keeping CS fixed and CL free generated the best-fit spectra. As is shown, except for spectrum 6b, all spectra could be fit with a very low percentage of the CS component, suggesting that the addition of Span80 to the PC liposomes maintains the relative stability of the structure while also stimulating lipid exchange with the SC membrane, whereas the other formulations retain more of the spin label since the spin label was already incorporated into their bilayers. It is expected that after a long period of incubation, the distribution of spin labels between the two environments (SC membranes and liposomes) reaches an equilibrium. The EPR spectra shown in Figs. 5 and 6 suggest that in the case of flexible liposomes, this equilibrium is displaced, i.e., a greater amount of probe is allocated to the SC membranes, and that the kinetics of the spin probe distribution are faster than in the case of the other liposomes. Analysis of the molecular dynamics of the CL shows a discreet increase in τ_c values for all studied liposomes.

4. Discussion

The EPR spectral best-fit method has been widely used to characterize and evaluate changes in the fluidity of the SC lipid lamellae

caused by permeation enhancers applied to the SC tissue (Anjos et al., 2007; dos Anjos and Alonso, 2008; de Queirós et al., 2005; dos Anjos et al., 2007; Alonso et al., 2012). In these cases, a marked increase in the molecular dynamics of the SC lipid matrix was observed. Alternatively, with the application of flexible liposomes and the other formulations used in the present study to the SC membranes, only moderate alterations in SC fluidity were observed. However, unlike the results for permeation enhancers, the EPR experimental spectrum of the SC membranes treated with flexible liposomes was characterized by the presence of two environments with very different lipid fluidities (Fig. 1).

Recently, Moraes et al. (2017) used EPR spectroscopy to investigate the interaction profile of an emulsified system with SC lipids that were spin-labeled with 5-DSA. The authors found an increase in the dynamics of the SC lipids (evidenced by a decrease of 5.3 G in the $2A_{||}$ parameter) when they were mixed with the emulsion. Moreover, the authors observed two completely distinct spectra for the spin label incorporated into a lamellar gel phase emulsion or the SC membranes. However, when the lipid emulsion was applied to the SC membranes, the resulting spectrum could not be described as a combination of two distinct mobility components, indicating that the spectrum was not the result of spin probes in two distinct microenvironments (SC and emulsion) but rather an interaction (fusion) between the formulation and SC lipids. Although our results showed different spectra for spin label 5-DSA incorporated into the intact SC intercellular membranes and the Span80-liposomal formulation, the application of Span80 liposomes to the SC membranes caused the resulting spectrum (Fig. 1d) to be a combination of the spectra of 5-DSA incorporated into both systems (combination of the 1a and 1b spectra). This result confirmed the interpretation that the liposome formulation remained relatively stable after mixing due to poor interactions with the SC membranes.

Spin label EPR data indicated that flexible liposomes are more fluid than pure PC liposomes. This increase in the dynamics of the flexible liposomes should be due to the presence of Span80 molecules as previously demonstrated using differential scanning calorimetry to examine the interactions of edge activators with DPPC membranes (El Maghraby et al., 2004). The authors concluded that in the presence of surfactants (including Span80), the packing of the liposome lipid bilayer changes in favor of the more fluid liposomes. On the other hand, the addition of cholesterol apparently induces a lateral and transverse order of the lipid chain segments, which leads to decreased spin label mobility (Kurad et al., 2004). In this study, cholesterol caused an increase of 1.5 G in the $2A_{||}$ (or ~0.5 ns for τ_c) values compared with those of pure PC liposomes (the spectrum of Fig. 4c). The SC lipids consist of an approximately equimolar ratio of fatty acids, ceramides and cholesterol (Weerheim and Ponec, 2001). In general, ceramides possess a sphingoid base combined with a (fatty acid) acyl chain, while fatty acids are predominantly saturated with a wide distribution of the chain lengths of both lipids (Van Smeden et al., 2014). Thus, the moderate decrease in the liposome bilayer fluidity could be ascribed to an exchange between the unsaturated PC lipids and the saturated SC lipids.

As reviewed by Sharma et al., the permeation efficiency of liposomes is intimately related to membrane fluidity (Sharma et al., 2014). In fact, *in vitro* skin permeability studies have demonstrated that the liquid-crystalline membrane phase confers better penetration to liposomes than does the gel phase (Ogiso et al.,1997). These results are consistent with our data, demonstrating that flexible liposomes, which have liquid-crystalline phase membranes, had more interactions with the SC membranes than the cholesterol formulations, which have liquid ordered phase membranes.

Several studies argue that the physicochemical features of liposomes modulate their efficiencies as drug carriers and that the addition of membrane-softening components, such as surfactants, ethanol or terpenes, can enhance vesicle elasticity and improve drug delivery (Cevc et al. 2002; Sharma et al., 2014). In this context, the incorporation of edge activators into liposome constituents led to enhanced flexibility and consequently increased skin penetration (Cevc and Vierl, 2010; Cevc, 2004; El Zaafarany et al., 2010). To date, two main penetration mechanisms for flexible liposome skin permeability have been proposed (Honeywell-Nguyen and Bouwstra, 2005). One claims that liposomes can act as drug carrier systems and that intact vesicles can penetrate SC membranes and deliver the entrapped drugs through the skin. The other mechanism proposes that due to their composition, flexible liposomes act as penetration enhancers, modifying the SC intercellular membrane fluidity and facilitating the penetration of the drug molecules into and across the membrane (Sharma et al., 2014). For instance, El Zaafarany and co-workers claim that Tween 80-PC flexible liposomes could facilitate *in vitro* permeation of diclofenac sodium (DS) in rabbit skin at twice the amount delivered by the marketed product Olfen® gel and that the residual amount of drug in the skin was nearly 5-times greater for flexible liposomes (El Zaafarany et al., 2010). The authors attributed the enhanced DS delivery to the ability of the flexible liposomes to act as both drug carriers and permeation enhancers. On the other hand, a very recent study using a combination of transmission electron microscopy and chromatographic and mass spectrometry demonstrated a relationship between the depth of human skin penetration and liposome flexibility in addition to observing intact liposomes in the epidermal layers, supporting the hypothesis of the whole vesicle penetration mechanism (Franzé et al., 2017). In fact, our results indicate the presence of two lipid environments with very distinct molecular dynamics in the flexible liposome-treated SC membranes and an important exchange of the spin probe. Thus, the alleged flexibility of the PC-Span80 formulation could improve the access of this type of liposome to the inner intercellular membranes of the SC and facilitate mutual lipid exchange.

5. Conclusions

An EPR spin labeling approach combined with a simulation methodology was used to demonstrate the coexistence of two distinct lipid domains with very different molecular dynamics in SC tissues treated with PC-Span80 flexible liposomes and other PC formulations (pure PC, PC + chol, PC + chol + DOTAP and PC + chol + DSPG). In terms of lipid fluidity, the flexible liposomes exhibited the highest fluidities and the liposomes containing cholesterol exhibited the lowest fluidities. None of the formulations significantly altered the SC membrane fluidity. Our results support the hypothesis of the whole vesicle skin penetration mechanism for the studied PC liposomes but showed that during the penetration process, an important exchange of a fatty acid spin label occurs between SC membranes and liposome lipids. When spin-labeled stearic acid was incorporated into the formulation prior to SC treatment, the amount of spin probe transferred to SC membranes was considerably higher for the flexible liposomes (PC + Span80), with an ~50% transference. However, when the SC was spin labeled prior to treatment, transfer of the probe from SC membranes to PC liposomes was lower with flexible liposomes (~40% transference). This exchange of lipids could be explored to modulate liposome integrity or SC lipid phase fluidity to decrease barrier function (in a reversible manner) and develop new and more effective liposomal carriers.

Conflict of interest statement

The authors declare no conflicts of interest.

Acknowledgments

This study was financially supported by grants from the Brazilian research funding agencies CNPq (445666/2014-5; 302216/2010-3, and 406521/2016-6), CAPES, and FAPEG (201210267001110 and PPP03/2015). All EPR measurements were performed on the spectrometer installed at the EPR Laboratory (UnB), which was acquired though the research support of CNPq (CNPq573.880/2008-5 – INCT

Nanobiotechnology).

References

Alonso, L., Mendanha, S.A., Marquezin, C.A., Berardi, M., Ito, A.S., Acuña, A.U., Alonso, A., 2012. Interaction of miltefosine with intercellular membranes of stratum corneum and biomimetic lipid vesicles. Int. J. Pharm. 434, 391–398. http://dx.doi.org/10.1016/j.ijpharm.2012.06.006.

Alonso, A., Vasques da Silva, J., Tabak, M., 2003. Hydration effects on the protein dynamics in stratum corneum as evaluated by EPR spectroscopy. Biochim. Biophys. Acta (BBA) - Proteins Proteomics 1646 (1), 32–41. http://dx.doi.org/10.1016/S1570-9639(02)00545-9.

Benson, H.A.E., 2017. Liposomes 1522, 107–117. http://dx.doi.org/10.1007/978-1-4939-6591-5.

Berliner, L.J., 1976. Spin Labeling: Theory and Applications. Academic Press.

Budil, D.E., Lee, S., Saxena, S., Freed, J.H., 1996. Nonlinear-least-squares analysis of slow-motion EPR spectra in one and two dimensions using a modified levenberg–marquardt algorithm. J. Magn. Reson., Ser. A 120 (2), 155–189. http://dx.doi.org/10.1006/jmra.1996.0113.

Camargos, H.S., Silva, A.H.M., Anjos, J.L.V., Alonso, A., 2010. Molecular dynamics and partitioning of di-tert-butyl nitroxide in stratum corneum membranes: effect of terpenes. Lipids 45 (5), 419–427. http://dx.doi.org/10.1007/s11745-010-3407-2.

Camargos, H.S., Moreira, R.A., Mendanha, S.A., Fernandes, K.S., Dorta, M.L., Alonso, A., 2014. Terpenes increase the lipid dynamics in the leishmania plasma membrane at concentrations similar to their IC50 values. PLoS One 9 (8), e104429. http://dx.doi.org/10.1371/journal.pone.0104429.

Cevc, G., 1996. Transfersomes, liposomes and other lipid suspensions on the skin: permeation enhancement, vesicle penetration, and transdermal drug delivery. Crit. Rev. Ther. Drug Carrier Syst. 13 (3–4), 257–388. http://dx.doi.org/10.1615/CritRevTherDrugCarrierSyst.v13.i3-4.30.

Cevc, G., 2004. Lipid vesicles and other colloids as drug carriers on the skin. Adv. Drug Delivery Rev. 56 (5), 675–711. http://dx.doi.org/10.1016/j.addr.2003.10.028.

Cevc, G., Gebauer, D., Stieber, J., Schätzlein, A., Blume, G., 1998. Ultraflexible vesicles, transfersomes, have an extremely low pore penetration resistance and transport therapeutic amounts of insulin across the intact mammalian skin. Biochim. Biophys. Acta - Biomembranes 1368 (2), 201–215. http://dx.doi.org/10.1016/S0005-2736(97)00177-6.

Cevc, G., Schätzlein, A., Richardsen, H., 2002. Ultradeformable lipid vesicles can penetrate the skin and other semi-permeable barriers unfragmented. Evidence from double label CLSM experiments and direct size measurements. Biochim. Biophys. Acta - Biomembranes 1564 (1), 21–30. http://dx.doi.org/10.1016/S0005-2736(02)00401-7.

Cevc, G., Vierl, U., 2010. Nanotechnology and the transdermal route: A state of the art review and critical appraisal. J. Control. Release 141 (3), 277–299. http://dx.doi.org/10.1016/j.jconrel.2009.10.016.

de Queirós, W.P., de Sousa Neto, D., Alonso, A., 2005. Dynamics and partitioning of spin-labeled stearates into the lipid domain of stratum corneum. J. Control. Release 106 (3), 374–385. http://dx.doi.org/10.1016/j.jconrel.2005.05.009.

dos Anjos, J.L.V., Alonso, A., 2008. Terpenes increase the partitioning and molecular dynamics of an amphipathic spin label in stratum corneum membranes. Int. J. Pharm. 350, 103–112. http://dx.doi.org/10.1016/j.ijpharm.2007.08.024.

dos Anjos, J.L.V., Neto, D.D.S., Alonso, A., 2007. Effects of ethanol/l-menthol on the dynamics and partitioning of spin-labeled lipids in the stratum corneum. Eur. J. Pharm. Biopharm. 67, 406–412. http://dx.doi.org/10.1016/j.ejpb.2007.02.004.

Anjos, J.L., Dos, V., Neto, D.D.S., Alonso, A., 2007. Effects of 1,8-cineole on the dynamics of lipids and proteins of stratum corneum. Int. J. Pharm. 345 (1–2), 81–87. http://dx.doi.org/10.1016/j.ijpharm.2007.05.041.

Duangjit, S., Obata, Y., Sano, H., Onuki, Y., Opanasopit, P., Ngawhirunpat, T., Takayama, K., 2014. Comparative study of novel ultradeformable liposomes: menthosomes, transfersomes and liposomes for enhancing skin permeation of meloxicam. Biol. Pharm. Bull. 37 (2), 239–247. http://dx.doi.org/10.1248/bpb.b13-00576.

El Maghraby, G.M., Williams, A., Barry, B., 2004. Interactions of surfactants (edge activators) and skin penetration enhancers with liposomes. Int. J. Pharm. 276 (1–2), 143–161. http://dx.doi.org/10.1016/j.ijpharm.2004.02.024.

El Maghraby, G.M., Barry, B.W., Williams, a.C., 2008. Liposomes and skin: From drug delivery to model membranes. Eur. J. Pharm. Sci. 34 (4–5), 203–222. http://dx.doi.org/10.1016/j.ejps.2008.05.002.

El Maghraby, G.M.M., Williams, A.C., Barry, B.W., 2006. Can drug-bearing liposomes penetrate intact skin? J. Pharm. Pharmacol. 58 (4), 415–429. http://dx.doi.org/10.1211/jpp.58.4.0001.

El Zaafarany, G.M., Awad, G.A.S., Holayel, S.M., Mortada, N.D., 2010. Role of edge activators and surface charge in developing ultradeformable vesicles with enhanced skin delivery. Int. J. Pharm. 397 (1–2), 164–172. http://dx.doi.org/10.1016/j.ijpharm.2010.06.034.

Elias, P.M., Brown, B.E., Fritsch, P., Goerke, J., Gray, G.M., White, R.J., 1979. Localization and composition of lipids in neonatal mouse stratum granulosum and stratum corneum. J, Invest. Dermatol. 73 (5), 339–348.

Elsayed, M.M.A., Abdallah, O.Y., Naggar, V.F., Khalafallah, N.M., 2007. Deformable liposomes and ethosomes as carriers for skin delivery of ketotifen. Pharmazie 62 (2), 133–137. http://dx.doi.org/10.1691/ph.2007.2.6082.

Franzé, S., Donadoni, G., Podestà, A., Procacci, P., Orioli, M., Carini, M., Cilurzo, F., 2017. Tuning the extent and depth of penetration of flexible liposomes in human skin. Mol. Pharm. 14 (6), 1998–2009. http://dx.doi.org/10.1021/acs.molpharmaceut.7b00099.

Honeywell-Nguyen, P.L., Bouwstra, J.A., 2005. Vesicles as a tool for transdermal and dermal delivery. Drug Discovery Today: Technol. 2 (1), 67–74. http://dx.doi.org/10.1016/j.ddtec.2005.05.003.

Karande, P., Jain, A., Ergun, K., Kispersky, V., Mitragotri, S., 2005. Design principles of chemical penetration enhancers for transdermal drug delivery. PNAS 102 (13), 4688–4693. http://dx.doi.org/10.1073/pnas.0501176102.

Kurad, D., Jeschke, G., Marsh, D., 2004. Lateral Ordering of Lipid Chains in Cholesterol-Containing Membranes: High-Field Spin-Label EPR. Biophys. J . 86 (1), 264–271. http://dx.doi.org/10.1016/S0006-3495(04)74102-8.

Malik, D.K., Baboota, S., Ahuja, A., Hasan, S., Ali, J., 2007. Recent advances in protein and peptide drug delivery systems. Curr Drug Delivery 4 (2), 141–151.

Mendanha, S.A., Alonso, A., 2015. Effects of terpenes on fluidity and lipid extraction in phospholipid membranes. Biophys. Chem. 198, 45–54. http://dx.doi.org/10.1016/j.bpc.2015.02.001.

Mendanha, S.A., Moura, S.S., Anjos, J.L.V.V., Valadares, M.C., Alonso, A., 2013. Toxicity of terpenes on fibroblast cells compared to their hemolytic potential and increase in erythrocyte membrane fluidity. Toxicol. In Vitro 27 (1), 323–329. http://dx.doi.org/10.1016/j.tiv.2012.08.022.

Mendanha, S.A., Marquezin, C.A., Ito, A.S., Alonso, A., 2017. Effects of nerolidol and limonene on stratum corneum membranes: a probe EPR and fluorescence spectroscopy study. Int. J. Pharm. 532 (1), 547–554. http://dx.doi.org/10.1016/j.ijpharm.2017.09.046.

Moraes, C., Anjos, J.L.V., Maruno, M., Alonso, A., Rocha-filho, P., 2017. Development of lamellar gel phase emulsion containing baru oil (dipteryx alata vog.) as a prospective delivery system for cutaneous application. Asian J. Pharm. Sci. http://dx.doi.org/10.1016/J.AJPS.2017.09.003.

Moreira, R.A., Mendanha, S.A., Fernandes, K.S., Matos, G.G., Alonso, L., Dorta, M.L., Alonso, A., 2014. Miltefosine increases lipid and protein dynamics in leishmania amazonensis membranes at concentrations similar to those needed for cytotoxicity activity. Antimicrob. Agents Chemother. 58 (6), 3021–3028. http://dx.doi.org/10.1128/AAC.01332-13.

Narishetty, S.T.K., Panchagnula, R., 2004. Transdermal delivery of zidovudine: effect of terpenes and their mechanism of action. J. Control. Release 95 (3), 367–379. http://dx.doi.org/10.1016/j.jconrel.2003.11.022.

Ogiso, T., Niinaka, N., Iwaki, M., Tanino, T., 1997. Mechanism for enhancement effect of lipid disperse system on percutaneous absorption. Int. J. Pharm. 152 (2), 135–144. http://dx.doi.org/10.1016/S0378-5173(97)04919-3.

Pilcer, G., Amighi, K., 2010. Formulation strategy and use of excipients in pulmonary drug delivery. Int. J. Pharm. 392 (1–2), 1–19. http://dx.doi.org/10.1016/j.ijpharm.2010.03.017.

Prausnitz, M.R., Langer, R., 2008. Transdermal drug delivery. Nat. Biotechnol. 26 (11), 1261–1268. http://dx.doi.org/10.1038/nbt.1504.

Prausnitz, M.R., Mitragotri, S., Langer, R., 2004. Current status and future potential of transdermal drug delivery. Nat. Rev. Drug Discovery 3 (2), 115–124. http://dx.doi.org/10.1038/nrd1304.

Sahoo, C.K., Nayak, P.K., Sarangi, D.K., Sahoo, T.K., 2013. Intra vaginal drug delivery system: an overview. Am. J. Adv. Drug Delivery 043–055. http://doi.org/ISSN-2321-547X.

Sharma, V.K., Sarwa, K.K., Mazumder, B., 2014. Fluidity enhancement: a critical factor for performance of liposomal transdermal drug delivery system. J. Liposome Res. 24 (2), 83–89. http://dx.doi.org/10.3109/08982104.2013.847956.

Touitou, E., Dayan, N., Bergelson, L., Godin, B., Eliaz, M., 2000. Ethosomes - Novel vesicular carriers for enhanced delivery: characterization and skin penetration properties. J. Control. Release 65 (3), 403–418. http://dx.doi.org/10.1016/S0168-3659(99)00222-9.

van Smeden, J., Janssens, M., Gooris, G.S., Bouwstra, J.A., 2014. The important role of stratum corneum lipids for the cutaneous barrier function. Biochim. Biophys. Acta (BBA) – Mol. Cell Biol. Lipids 1841 (3), 295–313. http://dx.doi.org/10.1016/j.bbalip.2013.11.006.

Weerheim, A., Ponec, M., 2001. Determination of stratum corneum lipid profile by tape stripping in combination with high-performance thin-layer chromatography. Arch. Dermatol. Res. 293 (4), 191–199. http://dx.doi.org/10.1007/s004030100212.